Generation of Description for Eye Fundus Desease

Elena Himbitskaya
Belarusian State University
Minsk, Belarus
Email: fpm.gimbicka@bsu.by

Vadim Ermakov
Belarusian State Medical University
Minsk, Belarus
Email: ermakouvv@gmail.com

Alexander Nedzved
Belarusian State University
United Institute of Informatics Problems NAS Belarus
Minsk, Belarus
Email: Anedzved@bsu.by

***Abstract*—This research proposes an algoritm for detecting and evaluating signs of optic nerve disc degeneration of various genesis. This algorithm is based on the analysis of a diagnostic protocol, which is built by extracting a semantic map from an ocular fundus image and analyzing the characteristics of object classes associated with the manifestations of opticoneuropathies.**

***Keywords*—automated model, ocular fundus, deep learning, convolutional neural network, segmentation**

I. Introduction

Optic nerve atrophy, accompanied by destruction of nerve fibres and progressing death of retinal ganglion cells (RGCs), is one of the most common causes of decreased visual function, up to complete blindness. Despite the variety of clinical manifestations, optic atrophy has a common feature — a change in the colour saturation of the optic nerve disc (OND). It has been discovered that this sign is most often detected before the appearance of functional disorders associated with the disease. In this case, pallor of the optic disc and replacement of its typical pink shades with grey tones turns out to be an indicator of a latently running disease [1]. The above is fully applicable to multiple sclerosis (MS) — a chronic progressive autoimmune-inflammatory and neurodegenerative disease characterized by the formation of multiple lesion foci mainly in the white matter of the central nevrous system (CNS) and progression of focal and diffuse brain atrophy [2]. It is shown that multiple sclerosis is accompanied by death of retinol ganglion cell axons and loss of visual functions. Early diagnosis of MS significantly increases the chances of long-term remission under the influence of medications that change the clinical course of the disease.

Various threshold methods measuring the degree of pallor of the RPE have been used to diagnose MS. However, when attempting to obtain generalized color characteristics, the objectivity of the results decreases, because this approach does not eliminate the dependencies on the settings and accuracy errors of the equipment used for photoregistration of the ocular fundus. The reliability of the result, in fact, remains within the limits of reliability of the results obtained by subjective, visual evaluation of the color of the optic nerve disc, which is currently used in practice [3].

Threshold method is quite suitable in cases of pronounced atrophy of the optic nerve disk, when the diagnosis is without a doubt. However, it is difficult to apply it in controversial cases when degenerative changes in the area of the neuroretinal rim of the optic nerve disc (pallor) have only initial or poorly expressed character. Meanwhile, detection of such changes is of special interest because, as it was mentioned above, degenerative changes can be detected much earlier than functional manifestations of pathologies (pallor of the neuroretinal rim) that caused these changes [4].

Fixation of the lesion zones, determination of their informatively significant characteristics [5] (which, apart from changes in color and shape of the OND, should include changes in the pattern of retinal vessels) can be performed with the help of the most advanced current methods of computer mathematics that use artificial intelligence — deep learning neural networks and mathematical models of machine learning [6].

The objective of the study is to develop an automated method for detecting and evaluating signs of optic disc degeneration of various genesis based on the analysis of a diagnostic protocol based on the spectrum of possible manifestations of optic neuropathies recorded on the surface of the optic disc [7]. The diagnostic protocol is compiled by extracting the semantic map of the ocular fundus image and analyzing the characteristics of class objects (manifestations of opticoneuropathies). The result of applying the voting algorithm to the diagnostic protocol of the image is then compared with the result of the developed neural network model that gives the assessment-diagnosis of multiple sclerosis.

II. Signs of different classes of neuropathies on ocular fundus images

Acquired atrophy can be due to two causes - compression of peripheral optic neurons (so-called primary form) or optic disc edema (so-called secondary form) [8].

A. Primary form

The primary or glaucomatous form of optic atrophy develops due to collapse of the lattice plate of the sclera which happens due to increased eye pressure. Glaucomatous optic neuropathy in the initial phase either does not cause pallor of the optic nerve disc at all, or the disc color change is very slight and can be spotted only in one segment. However, the development of the disease leads to the loss of ganglion cells, thinning of the optic disc and narrowing of the vessels of the eye fundus, as well as desolation and death of small vessels on the disc (Kestenbaum's symptom). A gradual thinning of the optic disc is happening. The pallor becomes more even, spreading over the entire surface of the disc. However, neither its shape nor size changes. A distinctive feature of glaucomatous neuropathy is the excavation zone increasing in size.

Although the growth of the excavation zone indicates the possible presence of pathology. But the size of excavation in healthy people is also variable: as a rule, a larger optic disc has a larger excavation zone, therefore, it is more important to assess the ratio of the optic disc size to the excavation zone. An increase in this ratio is most often evidence of abnormal contraction of glial cells. An important sign of pathology may be not only a change in the relative size of excavation, but also a difference in these parameters for two eyes.

B. Secondary form

The secondary form of atrophy is based on a pathological process in the optic disc itself, in which nerve fibers are replaced by neuroglia. In this case, there is a pronounced loss of pink shades of the optic disc neuroretinal rim, we can see disc swelling, its size increases, and its contours lose sharpness of borders.

Analysis of optic disc color should not be performed over the entire area, but only within the neuroretinal rim located in the area between the edge of the optic disc and the excavation zone. In this area ganglion cell axons are localized. In norm the color is pink and its change is a sign of retinal ganglion cells death. Blood vessels located in the optic disc area should also be excluded from the analysis of the color of the neuroretinal rim. Their selection as separate objects is necessary not only because they will influence the generalized color characteristics of the neuroretinal rim, but also because the condition of blood vessels is a diagnostic sign in itself. A decrease in the number of small blood vessels on the disc surface (Kestenbaum's sign), as well as weakening (thinning) of blood vessels around the disc may indicate the presence of pathology.

III. ResNet50 classifier for pathology detection

To realize the qualitative performance of the ResNet [9] classifier, the input parameters are tensors with dimensionality 16 x 256 x 256 x 256 x 3, where 16 is the batch size, 256 x 256 are the spatial dimensions of the images compatible with the neural network architecture, and 3 corresponds to the number of image channels. The model is trained and tested on a dataset of images obtained by semantic segmentation of the original images and containing classes of disk and excavation area and a region around the disk equal to its radius. The model contains 49 convolutional layers and defines 2 classes of pathology. Model's architecture is shown in Fig. 1.

Binary classification is performed using the Sigmoid function. After a fully connected layer, the values are brought to the range [0, 1], which means the probability of disease. A threshold = 0.5 is used for decision making and subsequent comparison with the true image label. The model was trained for 20 epochs with a gradual decrease in the learning rate parameter using torch.optimize.lr_scheduler. On the test data, the model concludes the diagnosis with 94% accuracy. Table I shows the error matrix for the test data on 203 patients.

Thus Recall of the model is about 0.95 and Precision is about 0.93.

Table I
Results as error matrix

Class	***Result***
TP (correctly predicted patient)	96
FN (incorrectly predicted healthy)	5
FP (incorrectly predicted sick)	7
TN (correctly predicted healthy)	101

IV. Semantic formation of disease description

According to our research to identify informative features for further analysis (as it is shown in Fig. 2) we should segment:

- neuroretinal rim;
- the excavation zone;
- blood vessels.

To form a semantic map of the image of informative objects (the optic nerve disk, excavation zone and vascular network) was chosen a convolutional neural network of Unet [10] architecture with a resnet18 backbone pretrained on the ImageNet dataset.

The model contains 23 convolutional layers and consists of convolutional (encoder) and up-convolutional (decoder) parts. To reduce each 64-component vector to the required number of classes, 1×1 convolutions are applied on the last layer. The input image size is determined by the need for even values of height and width for adequate application of subsampling operation (2×2 max pooling).

The network is trained by stochastic gradient descent based on the input images and their corresponding segmentation maps (masks). Applied function, soft-max

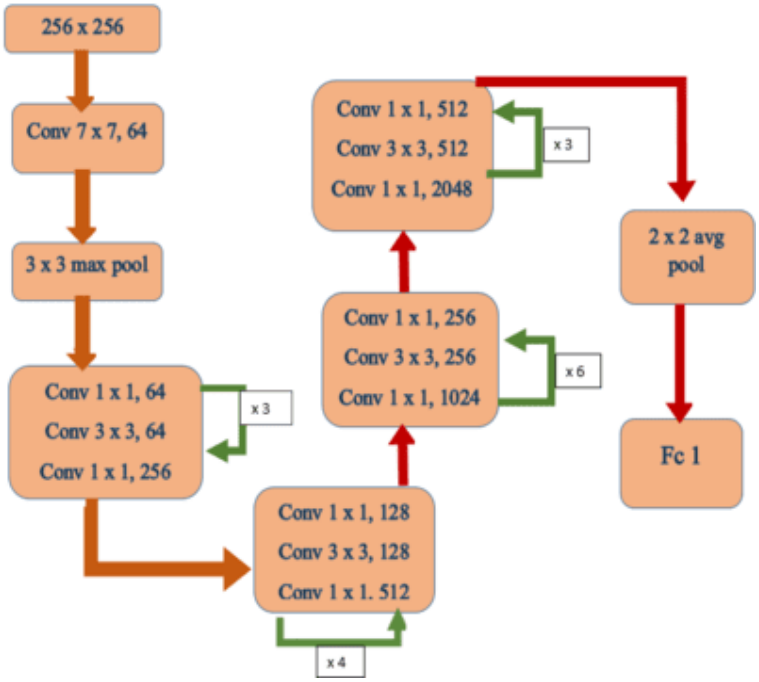

Figure 1. Classifier architecture.

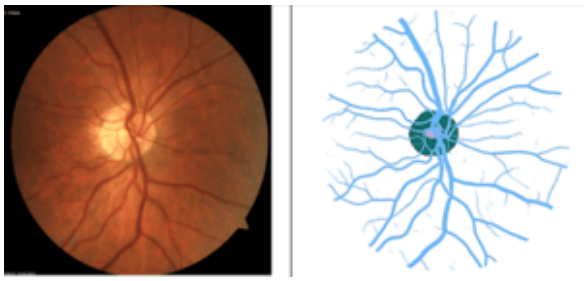

Figure 2. Semantic cart of an image.

brings the model prediction to the mask view. The loss function is a binary cross-entropy + jaccard functions. The accuracy is calculated by the BinaryIOU() [11] function, which finds the ratio of the correctly predicted mask to the union of the predicted and true masks.

A. *Segmentation of blood vessels*

The training of the model extracting the vascular network of the image was carried out in 2 stages. In the first stage, the network was trained on an additional set of 300 labeled data from publicly available datasets such as DRIVE [12], CHASE DB1 [13] and HRF [14]. In the second stage, the network was trained on target images.

Initially, the analyzed three-channel (RGB) image was compressed to a size of 996 x 996. After that, it was split into 9 slices with a resolution of 352 x 352 so that each slice captures a part of the neighboring slices (10 pixels). This is to eliminate distortion at the boundary between two tiles. Vessel segmentation by the neural network was performed for each tile. After the tiles were merged into a single image with the boundary 5 pixels cropped on each of them. They were then merged into rows. To smooth the transition between two tiles, their 5-pixel boundaries are overlaid and the resulting brightness is calculated using alpha blending to obtain a smooth transition. This process is shown in Fig. 3.

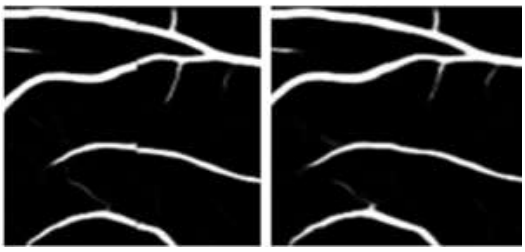

Figure 3. left — result of segmentation model on neighboring tiles, right — tiles merged with alpha blending

The same way the obtained 3 rows of tiles are combined into a vessel mask of the whole image. After that the obtained mask is stretched to the size of the original image.

The results of segmentation model for vascular network on training set and validation set are shown in Fig. 4 and their losses on training and validation set are shown in Fig. 5.

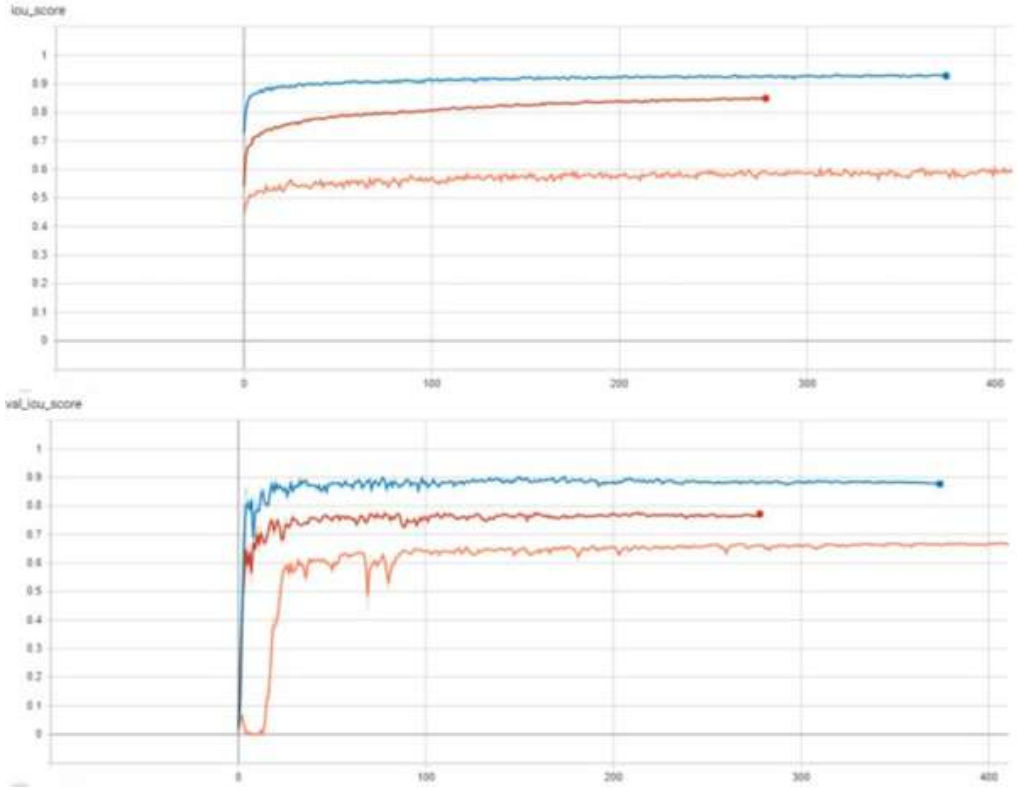

Figure 4. IoU score. first — training, second — validation. Blue — disk segmentation, red — excavation zone, orange — blood vessels

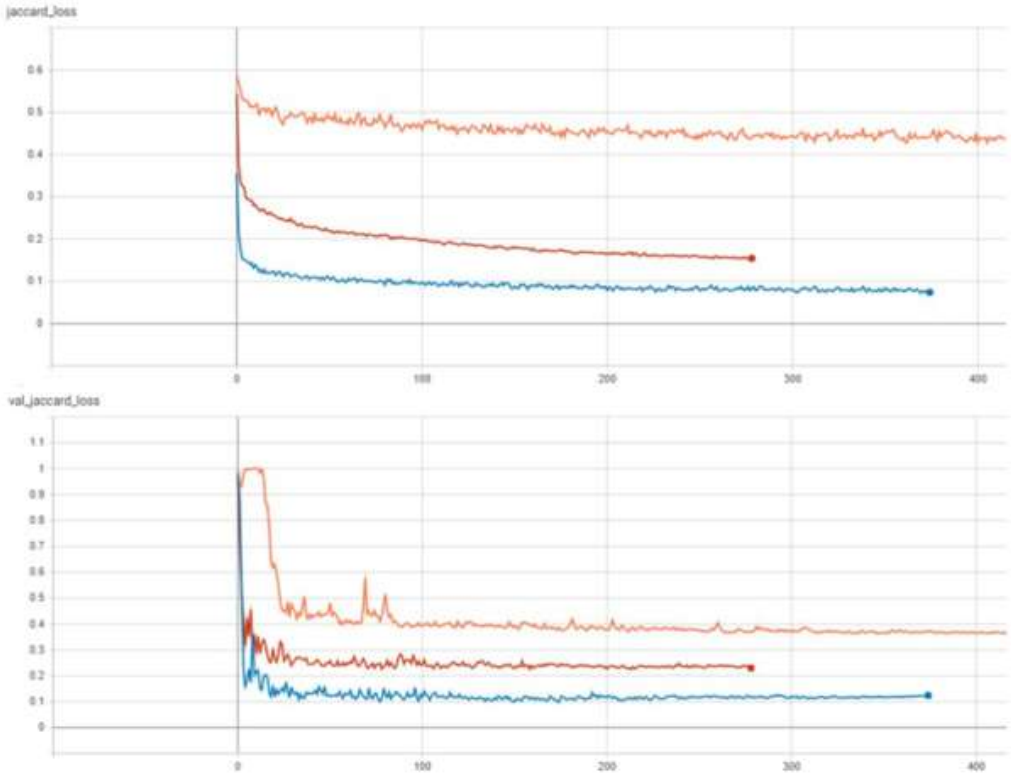

Figure 5. Jaccard loss. first — training, second — validation. Blue — disk segmentation, red — excavation zone, orange — blood vessels

B. Segmentation of optic nerve disk and excavation zone

Initially, the optic disc itself is segmented on the ocular fundus images compressed to a size of 352 x 352 using the same binary segmentation neural network (Fig. 6). The approximate radius of the disk is calculated, then the area of the original image containing the disk and having dimensions equal to three diameters of the disk is cut out. This image is transformed and used for segmentation of the excavation zone (Fig. 7).

The results of disk and excavation zone segmentation model on training set and validation set are shown in Fig. 4 and their losses on training and validation set are shown in Fig. 5.

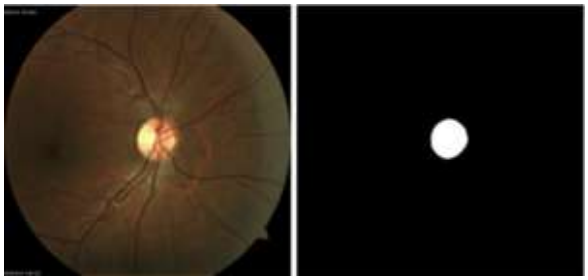

Figure 6. Image and mask of a disk

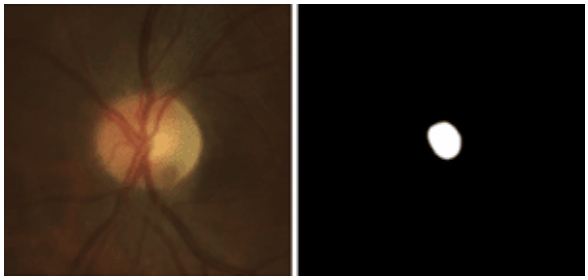

Figure 7. Image and mask of excavation zone

C. Signs of pathology manifestation

From the semantic segmentation map of these objects we need to extract such signs as:

- loss of clarity of the optic disc boundaries;
- enlargement of the cup in relation to the disk;
- Dying off of small vessels on the disk;
- branching characteristics of vessels.

Also from the provided image, should be extracted information about color signs of neuroretinal rim (disc area without excavation zone):

- graying of the neuroretinal rim (parameter H in HVS color model);
- graying of the neuroretinal rim (parameter S in HVS color model).

We should keep in mind that there is no clear relationship between these signs and the presence of early stage pathology, while at later stages of the disease the manifestation of primary optic atrophy increases, but perhaps the whole collection of signs will allow us to make some conclusions. Fig. 8 shows a scheme of the proposed automated method using the extracted features.

Now let's enlarge upon informative features and methods of their extraction. We will also consider methods of numerical expression of these signs.

1) Loss of clarity of the optic disc borders: Let's assume that this sign is manifested by the fact that the contour of the optic disc is clearer for images without pathology. To estimate the boundary clarity, we use the estimate of the intensity gradient on the contour and the variance of this gradient (Fig. 9), which is expected to be lower on the images with pathology. Specifically, we:

- extract the optic disc boundary obtained using the semantic map of the whole image as the image to be evaluated;
- apply the gradient operator, in our case the Sobel operator, to the boundary;
- calculate the total intensity gradient using the Euclidean norm of gradients along the horizontal and vertical axes.

2) The enlargement of the cup (excavation zone) relative to the disk: To estimate the enlargement of the cup (excavation zone) relative to the disk using information from the semantic map (Fig. 10), we calculate the ratio of the area of the excavation zone to the area of the optic nerve disk.

3) Dying off of small vessels on the disk: For this feature on the mask of the vascular network obtained from the semantic map, we will find and count the number of small vessels.

In this method, we will use the built-in functions of the cv2 library that remove "noise" in the image.

Let's assume that we call "small" vessels those that are less than 5 pixels wide. Then, taking them as noise, we use a kernel of 5 x 5 pixels to traverse the vascular network mask obtained from the semantic map and paint all small vessels. The obtained mask with only large vessels will be subtracted from the mask of all vessels and we will get only small vessels (Fig. 11).

4) Vascular network area: Calculating the area occupied by vessels can provide insight into the density and distribution of vessels. The method of measurement:

- counting all pixels that make up the vascular system. This can be done by simply counting the number of mask pixels that have a value corresponding to the vessel class;
- convert this number of pixels to area, given the scale of the image.

5) Vessel branching:

- we apply a skeletonization operation to the selected vessels to obtain their skeletal representation. In this

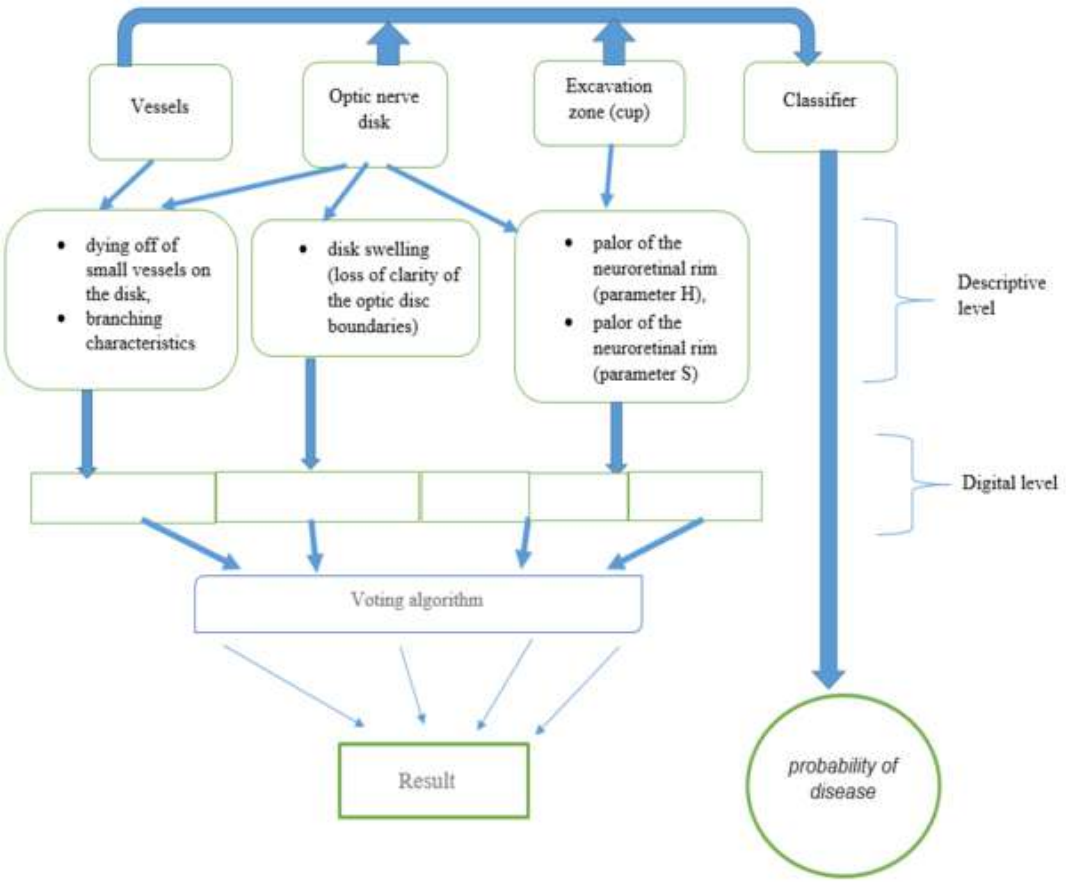

Figure 8. Pipeline of the automated method of semantic description generation for eyes diseases

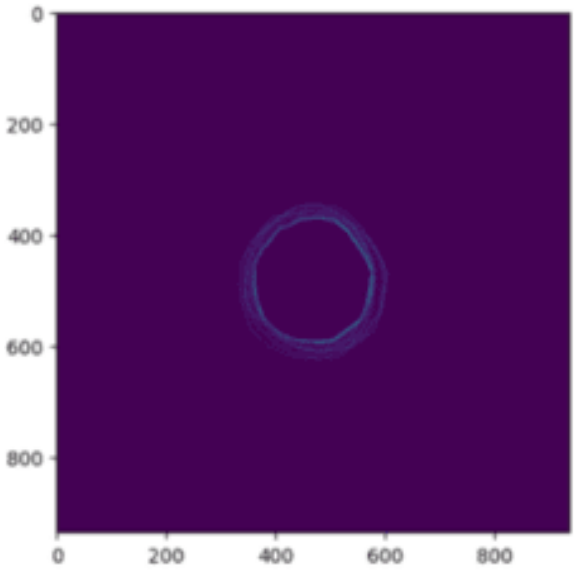

Figure 9. Mean gradient is 0.48. Gradient variance is 51

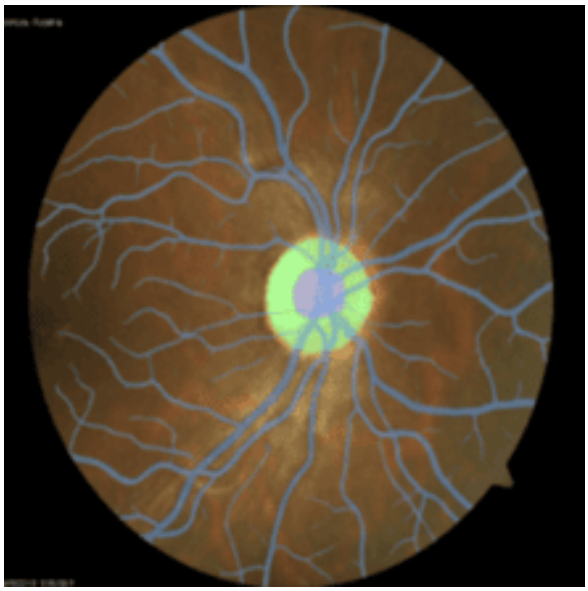

Figure 10. All classes highlighted

way, each vessel will be compressed to a width of 1 pixel;

- then for each pixel on the vessel skeleton, we perform the following steps:

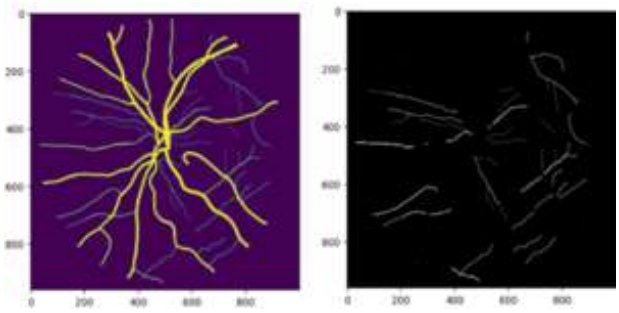

Figure 11. Small vessels extraction

  - define the 9-neighbor neighborhood of the pixel;
  - count the number of neighboring "active" pixels in the neighborhood;
  - if the number of neighboring "active" pixels is more than 3, it means that there is a branching of vessels in this place;
  - mark this pixel;
- since this algorithm can mark one branching several times, we will consider the number of connected marked components as the number of branching.
  Fig. 12 illustrates skeletonized vessel mask and it's branching points

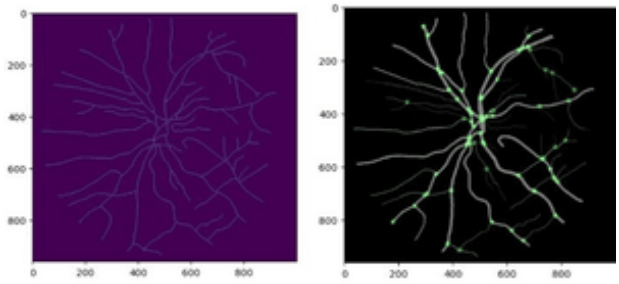

Figure 12. Number of branching points: 46

V. Conclusion

Systems capable of making semantic description for eyes diseases based on feature analysis represent a powerful tool for detecting and classifying pathologies. Such systems can be useful for monitoring and detecting early stages of different diseases.

However, we understand that the method requires additional research and validation on more diverse clinical data. It is also important to keep in mind that the final decision and diagnosis should always be based on a combination of data, expertise and clinical context.

Acknowledgment

The authors would like to thank the group of Laboratory of Information and Computer Technologies of Belarusian State Medical University for their valuable comments and help with data collecting, in particular, Grigory Karapetyan and Kosik Ivan.

References

[1] Ambika Selvakumar. Understanding Optic Disc Pallor - Shades of White. Mode of access: https://www.eophtha.com/posts/understanding-optic-disc-pallor-shades-of-white. – Date of access: accessed 24, Jan.

[2] Massimo Filippi, Amit Bar-Or, Fredrik Piehl, Alessandra Solari, Sandra Vukusic, Maria A. Rocca Multiple sclerosis. *Nature Reviews Disease Primers*, 2018, volume 4, Article number: 43.

[3] Shahzaib Iqbal, Tariq M. Khan, Khuram Naveed, Syed S. Naqvi, Syed Junaid Nawaz Recent trends and advances in fundus image analysis: A review. *Computers in Biology and Medicine*, 2022, Volume 151, Part A.

[4] Starovoitov V. V., Golub Y. I., Lukashevich M. M. Digital fundus image quality assessment. *System analysis and applied information science*, 2021, Volume 4, pp. 25–38.

[5] Bonilha VL. Age and disease-related structural changes in the retinal pigment epithelium. *Clin Ophthalmol*, 2008 Jun, vol. 2, no. 2, pp. 413–424. [Online]. Available: doi: 10.2147/opth.s2151

[6] Rohit Thanki A deep neural network and machine learning approach for retinal fundus image classification. *Healthcare Analytics*, 2023, vol. 3, 100140. [Online]. Available: doi: https://doi.org/10.1016/j.health.2023.100140

[7] Sarkar P, Mehtani A, Gandhi HC, Dubey V, Tembhurde PM, Gupta MK. Atypical optic neuritis: An overview. *Indian J Ophthalmol*, 2021 Jan, vol. 69 (1). [Online]. Available: doi: 10.4103/ijo.IJO_451_20

[8] T. S. Teleusova, M. M. Lepesova, A. L. Glaznye proyavleniya rasseyannogo skleroza [Ocular manifestations of multiple sclerosis]. *Vestnik AGIUV [Bulletin of the ASMRI]*, 2014, №3, pp 46-50.

[9] Liang, Jiazhi Image classification based on RESNET. *Journal of Physics: Conference Series*, 2020, 1634, 012110. [Online]. Available: doi: 10.1088/1742-6596/1634/1/012110

[10] Suri, Jasjit and Bhagawati, Mrinalini and Agarwal, Sushant and Paul, Sudip and Pandey, Amit and Gupta, Suneet and Saba, Luca and Paraskevas, Kosmas and Khanna, Narendra and Laird, John and Johri, Amer and Kalra, Manudeep and Fouda, Mostafa and Fatemi, Mostafa and Naidu, Desineni UNet Deep Learning Architecture for Segmentation of Vascular and Non-Vascular Images: A Microscopic Look at UNet Components Buffered With Pruning, Explainable Artificial Intelligence, and Bias. *IEEE Access*, 2022.[Online]. Available: doi: 10.1109/ACCESS.2022.3232561

[11] Adrian Rosebrock, Deep Learning for Computer Vision, PyImageSearch, 2017, 330 p.

[12] Paperswithcode. Available at: https://paperswithcode.com/dataset/drive

[13] Paperswithcode. Available at: https://paperswithcode.com/dataset/chase-db1

[14] Paperswithcode. Available at: https://paperswithcode.com/dataset/hrf

ГЕНЕРАЦИЯ ОПИСАНИЯ ДЛЯ ЗАБОЛЕВАНИЯ ГЛАЗНОГО ДНА

Гимбицкая Е. В., Ермаков В. В.,
Недзведь А. М.

В данной работе предлагается алгоритм для детекции и оценки клинических проявлений рассеянного склероза на снимках фундус-камерой глазного дна. Так как симптомы заболевания проявляются на различных объектах снимка, с помощью создания семантической карты исходного изображения, для каждого отдельного объекта оцениваются проявления симптомов. В результате работы данного алгоритма составляется диагностический протокол снимка. Далее полученный протокол можно сравнить с результатом модели-классификатора, работающей только с областью диска и оценивающей вероятность заболевания.

Received 19.03.2024